Antenna Effect in Highly Luminescent Eu^{3+} Anchored in Hexagonal Mesoporous Silica

Edimar DeOliveira,[†] Cláudio R. Neri,[†] Osvaldo A. Serra,*[,†] and Alexandre G. S. Prado[‡]

Laboratório de Terras Raras, Departamento de Química, FFCLRP, Universidade de São Paulo, Av. dos Bandeirantes 3900, 14040-901 Ribeirão Preto, São Paulo, Brazil, and Instituto de Química, Universidade de Brasília, Caixa Postal 4478, 70904-970 Brasília, Distrito Federal, Brazil

Received July 24, 2007

A route for coordination of Eu^{3+} by dibenzoylmethane (DBM) covalently bonded inside hexagonal mesoporous silica was established here to produce the highly luminescent nanomaterial SiDBM−Eu-$(DBM)_2$. Thermogravimetry, luminescence, X-ray diffraction, N_2 adsorption, FTIR, FTRaman, ^{29}Si NMR, and ^{13}C NMR in solid-state techniques were used to characterize SiDBM−Eu$(DBM)_2$. The ^{29}Si NMR spectrum proved that the DBM was covalently bonded to a silica framework. Thermogravimetric and titration data showed the 6.4×10^{-2} mmol of Eu^{3+} per gram of silica, and each Eu^{3+} is coordinated by three DBMs in SiDBM−Eu$(DBM)_2$. SEM images confirmed that this material is formed by nanoaggregates with 200 nm diameter. N_2 adsorption isotherms showed the SiDBM−Eu$(DBM)_2$ complex with 800 m^2 g^{-1} and 6.4 nm of porous diameter, characterizing mesoporosity of this nanomaterial. SiDBM−Eu$(DBM)_2$ showed an efficient DBM to Eu^{3+} intramolecular energy process, namely, antenna effect, which favored a highly luminescent behavior in this modified hexagonal mesoporous silica.

Introduction

Lanthanide complexes are an important class of compounds in the development of advanced luminescent materials and photoelectronic applications[1,2] such as laser materials[3] and luminescence labels[4,5] and in efficient light-conversion molecular devices (LCMDs),[6,7] organic light-emitting devices (OLEDs),[8] fluorescent lamps and cathode-ray tubes,[9] and plasma display panels (PDPs).[10] These complexes present sharp and intense emission lines upon ultraviolet light irradiation due to the lanthanide-centered luminescence generated from the effective intramolecular energy transfer from the coordinated ligands to the central lanthanide ion. This process is known as "antenna effect".[11,12]

Luminescence properties of lanthanides organic complexes anchored onto solid surfaces have been highlighted because of the photophysical properties that can be modified by the interaction between host and structure.[13,14] In this sense, Langmuir−Blodgett films,[15] porous glasses,[16] oxide surfaces,[17] and sol−gel glasses[18] have been applied as hosts for anchoring many lanthanides complexes. Recently, development of highly luminescent materials obtained by immobilization of lanthanides in organic/inorganic core−shell micro- or nanostructured particles have been extensively studied.[19−21] These particles show a quantum confinement effect which generates distinct optoelectronic properties that depends strongly on the particle size in the nanometer range.[22−24]

Taking into account that the supramolecular-templated mesostructured materials can be well-structured when a template such as a neutral polar molecule dispersed in water as micelles are disposed, during the sol−gel process, a new

* Corresponding author. E-mail: osaserra@usp.br.
† Universidade de São Paulo.
‡ Universidade de Brasília.

(1) Meng, Q.; Boutinaud, P.; Zhang, H.; Mahiou, R. *J. Lumin.* **2007**, *124*, 15.
(2) Li, H. R.; Lin, J.; Zhang, H. J.; Fu, L. S.; Meng, Q. G.; Wang, S. B. *Chem. Mater.* **2002**, *14*, 3651.
(3) Yokoyama, H. *Science* **1992**, *256*, 66.
(4) Richardson, F. S. *Chem. Rev.* **1982**, *82*, 541.
(5) Buonocore, G. E.; Li, H.; Marciniak, B. *Coord. Chem. Rev.* **1990**, *99*, 55.
(6) Li, S.; Song, H.; Li, W.; Ren, X.; Lu, S.; Pan, G.; Fan, L.; Yu, H.; Zhang, H.; Qin, R.; Dai, Q.; Wang, T. *J. Phys. Chem. B* **2006**, *110*, 23164.
(7) Farias, R. F.; Alves, S., Jr.; Belian, M. F.; Sá, G. F. *J. Colloid Interface Sci.* **2001**, *243*, 523.
(8) Zheng, Y.; Fu, L.; Zhou, Y.; Yu, J.; Yu, Y.; Wang, S.; Zhang, H. *J. Mater. Chem.* **2002**, *12*, 919.
(9) Zhang, W.; Zhang, W.; Xie, P.; Yin, M.; Chen, H.; Jing, L.; Zhang, Y.; Lou, L.; Xia, S. *J. Colloid Interface Sci.* **2003**, *262*, 588.
(10) Ronda, C. R. *J. Lumin.* **1997**, *72*, 49.
(11) Kłonkowski, A. M.; Lis, S.; Pietraszkiewicz, M.; Hnatejko, Z.; Czarnobaj, K.; Elbanowski, M. *Chem. Mater.* **2003**, *15*, 656.
(12) Sabbatini, N.; Guardigli, M.; Manet, I.; Ungaro, R.; Casnati, A.; Ziessel, R.; Uldrich, G.; Asfari, Z.; Lehn, J. M. *Pure Appl. Chem.* **1995**, *67*, 135.
(13) Tan, M.; Ye, Z.; Wang, G.; Yuan, J. *Chem. Mater.* **2004**, *16*, 2494.
(14) Nassar, E. J.; Neri, C. R.; Calefi, P. S.; Serra, O. A. *J. Non-Cryst. Solids* **1999**, *247*, 124.
(15) Serra, O. A.; Rosa, I. L. V.; Medeiros, C. L.; Zaniquelli, M. E. D. *J. Lumin.* **1994**, *60*, 112.
(16) Avnir, D.; Levy, D.; Reisfeld, R. *J. Phys. Chem.* **1984**, *88*, 5956.
(17) Zhang, J.; Gao, G.; Zhang, M.; Zhang, D.; Wang, C.; Zhao, D.; Liu, F. *J. Colloid Interface Sci.* **2006**, *301*, 78.
(18) Matthews, L. R.; Knobbe, E. T. *Chem. Mater.* **1993**, *5*, 1697.
(19) Liu, G.; Hong, G.; Sun, D. *J. Colloid Interface Sci.* **2004**, *278*, 133.
(20) Bazzi, R.; Flores, M. A.; Louis, C.; Lebbou, K.; Zhang, W.; Dujardin, C.; Roux, S.; Mercier, B.; Ledoux, G.; Bernstein, E.; Perriat, P.; Tillement, O. *J. Colloid Interface Sci.* **2004**, *273*, 191.
(21) Meng, Q. G.; Boutinaud, P.; Franville, A. C.; Zhang, H. J.; Mahiou, R. *Microporous Mesoporous Mater.* **2003**, *65*, 127.
(22) Gomes, J.; Pires, A. M.; Serra, O. A. *J. Fluoresc.* **2006**, *16*, 411.
(23) Sun, S.; Murray, C. B. *J. Appl. Phys.* **1999**, *85*, 4325.
(24) Wang, W.; Widiyastuti, W.; Ogi, T.; Lenggoro, I. W.; Okuyama, K. *Chem. Mater.* **2007**, *19*, 1723.

10.1021/cm701997y CCC: $37.00
Published on Web 10/09/2007

material with highly ordered pores can be formed.[25−28] Thus, Eu^{3+} chelate with β-diketonate anchored in the pores of hexagonal mesoporous silica was synthesized and its luminescence behavior was reported in this paper.

Experimental Section

2.1. Chemicals. The silica source for the inorganic framework formation was derived from tetraethylorthosilicate, TEOS (Acros). The silylant agent, 3-chloropropyltrimethoxysilane, SiCl (Sigma), dibenzoylmethane, DBM (Aldrich), the surfactant *n*-dodecylamine (Sigma), europium oxide (Aldrich), hydrochloric acid (Vetec), and methanol and ethanol (Aldrich) were all reagent grade.

2.2. Preparation of Sodium β-Diketonate (DBM−Na). $Na_{(s)}$ (0.23 g, 10.0 mmol) was dissolved in 30 mL of ethanol under an argon atmosphere to produce sodium ethoxide. To this solution were added 2.02 g (9.0 mmol) of DBM and 25 mL of anidryde ether. This solution was stocked overnight at 5 °C. Subsequently, the suspension was washed with anidryde ether and the solvent was removed by rotoevaporation, producing DBM−Na.[29]

2.3. Synthesis of Pendant Group. SiCl (1.09 mL, 6.0 mmol) and 1.47 g (6.0 mmol) of DBM−Na were added to 10 mL of methanol. The solution was stirred mechanically under a dry argon atmosphere at 50 °C for 24 h. The new silylant agent was denoted as PDBM−Na.

2.4. Modified HMS Synthesis. The new hexagonal mesoporous silica was prepared by stirring 3.33 g (18.0 mmol) of *n*-dodecylamine in 150 mL of water/ethanol (3:1 v/v) for 30 min until an opalescent solution was obtained, as a consequence of micelle formation.[30] TEOS (5.35 mL, 24.0 mmol) and 10 mL of methanol solution containing the organosilane PDBM−Na prepared above were added to the micellar suspension. This suspension was stirred for 48 h at room temperature, resulting in a precipitate that was removed by filtration. The *n*-dodecylamine inside the pores of the synthesized compound was extracted with ethanol at reflux temperature for 72 h in a Soxhlet system, producing the final product (SiDBM−Na).

2.5. Anchoring of Eu^{3+} by SiDBM−Na. SiDBM−Na (0.30 g) and 2.35 mL of $EuCl_3$ (0.10 mol L^{-1}) were suspended in 10 mL of ethanol, producing SiDBM−Eu. To complete the coordination sphere of Eu^{3+}, Si−DBMEu (50 mg) was suspended with 20 mg of DBM−Na in 5 mL of ethanol to produce the final luminescent material, SiDBM−$Eu(DBM)_2$.

2.6. Characterization. The amount of europium complexed by SiDBM−Na was determined by titration with EDTA using xilenol orange indicator, as described in the literature.[31]

Thermogravimetric analysis of the sample materials was followed in a TA Instruments SDT 2960 simultaneously in air flux with a heating rate of 10 °C/min, from room temperature to 850 °C.

Infrared spectra of all samples were performed on KBr pellets in the 4000−400 cm^{-1} region with a resolution of 4 cm^{-1}, by accumulating 64 scans using a Perkin-Elmer FTIR 1600.

FT-Raman spectra of the solid samples were obtained on a Bruker Equinox 55 equipped with a Raman accessory. The resulting spectra were the sum of 128 scans and the laser power was set at 300 mW. The spectral resolution was 4 cm^{-1}.

^{29}Si and ^{13}C nuclear magnetic resonance spectra of the solid sample were obtained on a Bruker AC 300 NMR spectrometer at room temperature. For each run, approximately 1 g of the catalyst was compacted into a 7 mm double bearing zirconia rotor. The measurements were obtained at frequencies of 75.47 and 59.61 MHz for carbon and silicon, respectively, with a magic-angle spinning speed of 3 kHz. To increase the signal-to-noise ratio of the solid-state spectra, the CP/MAS technique was used to obtain ^{29}Si and ^{13}C spectra, with pulse repetitions of 1 and 2 s and contact times of 1 and 4 ms, respectively.

Scanning electron microscopy (SEM) images were carried out on a Zeiss EVO 50; samples were coated with a gold film in a controlled deposition by using a Sputter Coater Baltec SCD 050.

Nitrogen adsorption−desorption data were acquired on a Quantachrome Nova 2200 analyzer, at 77 K. The surface area was calculated by the Brunauer−Emmett−Teller (BET) method, and pore size distribution was derived from the adsorption branches of the isotherms using the Barrett−Joyner−Halenda (BJH) method.

Powder X-ray diffraction (XRD) patterns were measured on a D 5005 X-SIEMENS diffractometer using Cu Kα radiation.

The excitation and emission spectra of the samples were obtained with a SPEX TRIAX - FLUOROLOG III spectrofluorimeter, at room temperature. Luminescence lifetimes were obtained with the accessory 1934D phosphorimeter with a pulsed xenon lamp.

Results and Discussion

3.1. Synthesis of Luminescent Hexagonal Mesoporous Silica SiDBM−$Eu(DBM)_2$. An overview on the progress of the inorganic surface immobilization field is closely related to the advancement of the synthetic chemistry involved. The key features associated with this subject can cause expansion or insertion of the main organic chain precursor silylating agent, by exploring the presence of reactive centers on it.[32−34] The employed precursor (SiCl) was available to react with DBM−Na according to eq 1 to produce the new pendant group (PDBM−Na). This new silane was used with the aim of modifying the hexagonal mesoporous silica.

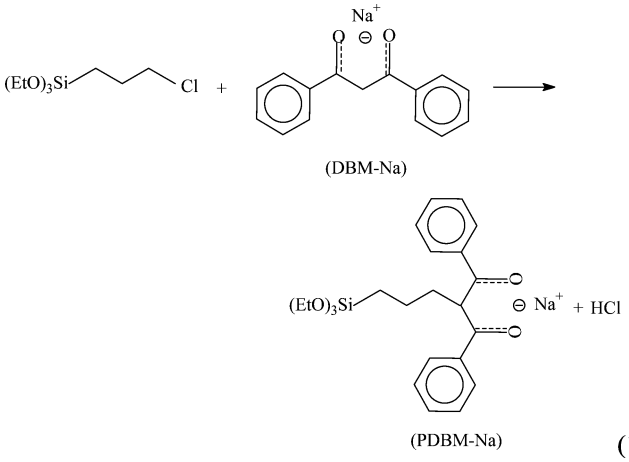

(1)

(25) Prado, A. G. S.; DeOliviera, E. *J. Colloid Interface Sci.* **2005**, *291*, 53.
(26) Prado, A. G. S.; Airoldi, C. *J. Mater. Chem.* **2002**, *12*, 3823.
(27) Macquarrie, D. J. *Philos. Trans. R. Soc. London, Ser. A* **2000**, *358*, 419.
(28) Evangelista, S. M.; DeOliveira, E.; Castro, G. R.; Zara, L. F.; Prado, A. G. S. *Surf. Sci.* **2007**, *601*, 2194.
(29) West, R.; Riley, R. *J. Inorg. Nucl. Chem.* **1958**, *5*, 295.
(30) Sales, J. A. A.; Prado, A. G. S.; Airoldi, C. *Surf. Sci.* **2005**, *590*, 51.
(31) Lyle, S. J.; Rahman, M. *Talanta* **1963**, *10*, 1177.
(32) DeOliveira, E.; Torres, J. D.; Silva, C. C.; Luz, A. A. M.; Bakuzis, P.; Prado, A. G. S. *J. Braz. Chem. Soc.* **2006**, *17*, 994.
(33) Tanev, P. T.; Pinnavaia, T. J. *Chem. Mater.* **1996**, *8*, 2068.
(34) Serra, O. A.; Nassar, E. J.; Rosa, I. L. V. *J. Lumin.* **1997**, *72−74*, 263.

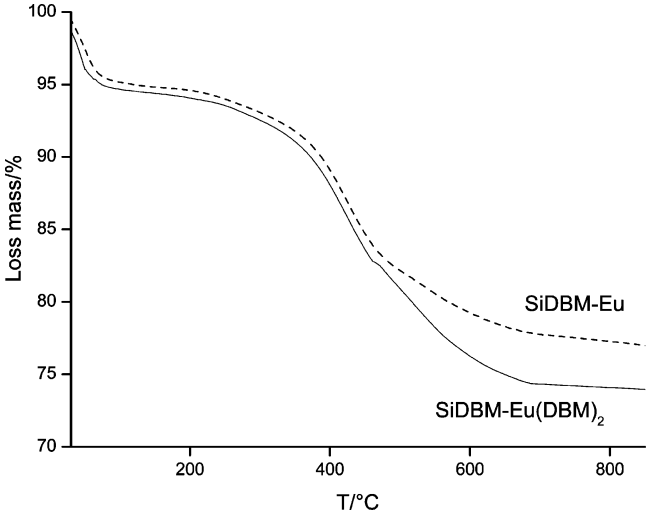

Figure 1. TG curves of SiDBM−Eu and SiDBM−$Eu(DBM)_2$.

Table 1. Thermogravimetric Data of SiDBM−Eu and SiDBM−$Eu(DBM)_2$

	Δm/%	ΔT/°C
SiDBM−Eu	4.78	30−180
	17.43	180−800
SiDBM−$Eu(DBM)_2$	4.49	30−180
	20.14	180−800

To obtain modified mesoporous hexagonal silica, the presence of *n*-dodecylamine, a molecule that contains a polar head and a long nonpolar hydrocarbon tail, enables the formation of a convenient experimental micellar condition in water. This molecular arrangement favors the tetraethoxysilane compound in the hydrolyzing process, together with the presence of the silylating agents PDBM−Na causes an inorganic polymeric backbone formation in an organized form around the micelles. With such organization, the amine groups of the *n*-dodecylamine molecules are directed to the available silanol groups and the corresponding pendant groups are maintained around the micelles. These structured silanol−surfactant interactions can be explained from electrostatic and hydrogen bond formation processes. Thus, both silylating agents can yield inorganic−organic mesoporous hybrids after polymerization, starting from TEOS molecules around the micelle previously formed by *n*-dodecylamine in water. After this synthesis, template was removed by ethanol reflux, forming the modified mesoporous hexagonal silica named SiDBM−Na. This silica reacted with $EuCl_3$ to form SiDBM−Eu. Finally, SiDBM−Eu was reacted with of DBM−Na to produce SiDBM−$Eu(DBM)_2$, according to eq 2.

3.2. Characterization of Material. Complexometric titration of the digested SiDBM−$Eu(DBM)_2$ showed that the 6.4×10^{-2} mmol of Eu^{3+} is present in each gram of silica. Thermogravimetric analysis of SiDBM−Eu and SiDBM−$Eu(DBM)_2$ was carried out to understand the coordination of the organic pendant group bonded to the hexagonal mesoporous silica.

Thermogravimetric curves (Figure 1) showed two distinct stages of decomposition. The one between 30 and 180 °C was related to adsorbed water and other one between 180 and 800 °C was assigned to decomposition of organic matter

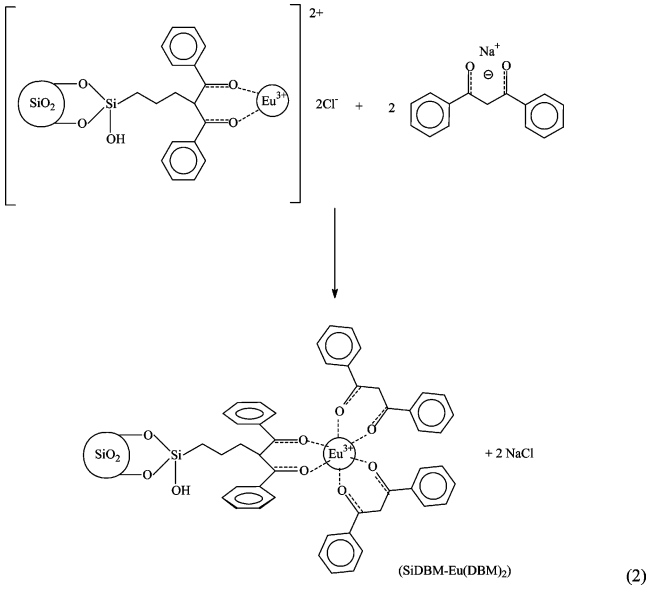

(2)

and water from sylanol groups condensation. The detailed thermogravimetric data are presented in Table 1. From the data on the organic matter decomposition, the amount of DBM present in the materials was determined. SiDBM−Eu presented 0.67 mmol of DBM per gram of material. This result shows that this material presents a total of 10.6 DBM groups per each Eu^{3+}. On the other hand, thermogravimetric data of SiDBM−$Eu(DBM)_2$ showed the increasing of 0.121 mmol of DBM per gram of material. Taking into account the presence of 6.4×10^{-2} mmol of Eu^{3+} per gram of material, thermogravimetric data showed the presence of 2.91 bonded DBM molecules per each Eu^{3+}, confirming the existence of Eu^{3+} coordinated by 3 DBMs according to eq 2.

FTIR and FTRaman (Figures 2 and 3) showed characteristic peaks of DBM and silica in the spectra.

FTIR spectra of DBM and SiDBM−$Eu(DBM)_2$ (Figure 2) presented the typical bands of DBM and silica structure, such as a large band between 3600 and 2800 cm^{-1} assigned to OH stretching of silanol groups of inorganic structure of material, and also adsorbed and bonded water.[33] Two peaks at 2984 and 2850 cm^{-1} are related to C−H stretching of sp^3 carbon. An intense band at 1070 cm^{-1} can be observed and is assigned to an asymmetric stretching of siloxane groups.[33] Signals related to DBM pendant group bonded to silica framework can also be observed in the FTIR and FTRaman spectra. Broad peaks between 1630 and 1317 cm^{-1} were related to (OCCCO) stretchings of DBM before and after the Eu^{3+} chelation.[35] Detailed vibration data are presented in Table 2.

SEM images were carried out to understand the morphology of SiDBM−$Eu(DBM)_2$ particles (Figure 4). These images showed that SiDBM−$Eu(DBM)_2$ presents a high level of aggregation caused by supramolecular formation of the hydrogen bonds among the silanol groups of silica particles. The images also showed that the supramolecular aggregates present 100 nm radius, thus characterizing a nanosized material.

(35) Prado, A. G. S.; Sales, J. A. A.; Carvalho, R. M.; Rubim, J. C.; Airoldi, C. *J. Non-Cryst. Solids* **2004**, *333*, 61.

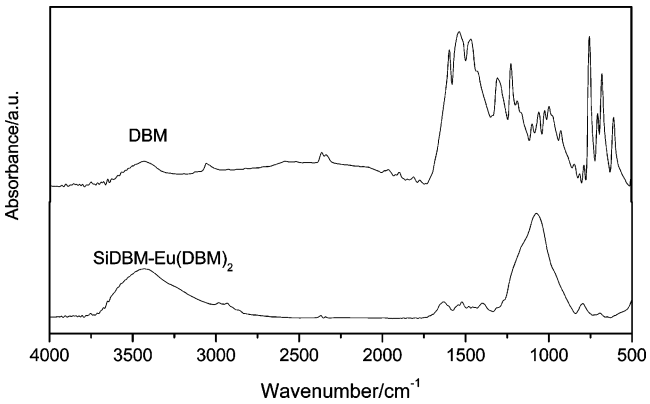

Figure 2. FTIR spectra of DBM and SiDBM−Eu(DBM)$_2$.

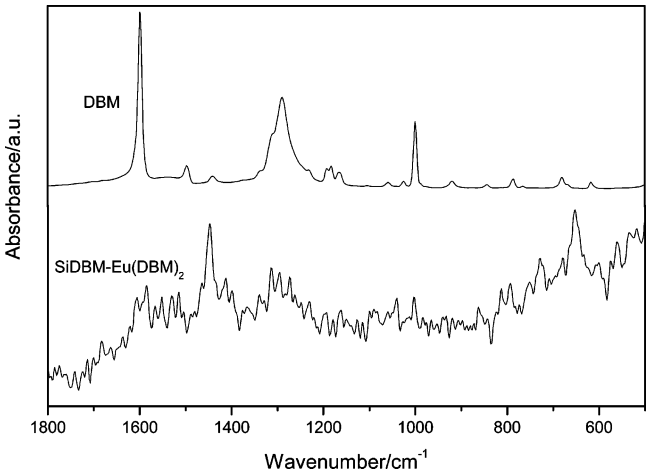

Figure 3. FTRaman spectra of DBM and SiDBM−Eu(DBM)$_2$.

Table 2. Wavenumbers Observed in FT-Raman Spectra of the Investigated Samples and the Respective Vibrational Assignments

SiDBM−Eu(DBM)$_2$		DBM		
IR	Raman	IR	Raman	description
3425		3450		ν(O−H)
		3050	3050	$\nu(C_{sp2}-H)$
2979	2979	2934	2934	$\nu(C_{sp3}-H)$
2928	2928			$\nu(C_{sp3}-H)$
2850	2850			$\nu(C_{sp3}-H)$
1631		1598	1598	ν_{as}(C═O)
	1293−1273	1288	1288	$\phi\nu$(C−C)
1523	1523	1545		ν (C═C)
	1445	1458		ν_s(C═O)
1404				δ(C−H)
		1311		*$\phi\nu$(C−C)*
1070	1070			ν(Si−O−Si)
945	945			*ν(Si−OH)*
748	748			*ϕ(Si−O−Si)*

Nitrogen adsorption−desorption isotherms obtained for SiDBM−Eu(DBM)$_2$ (Figure 5) show that the adsorption−desorption process is not reversible. This is a consequence of the hysteresis loops caused by the useful and unambiguous relation between the pressure of the capillary condensation and the pore size.[36−38] The isotherm is reversible up to a relative pressure of about 0.30. Irreversibility can be observed in the case of the samples where the condensation in primary mesopores takes place slightly above the latter pressure limit between relative pressures of 0.3 and 0.9. In summary, the BET surface area of the material is 800 m^2 g^{-1}, and the BJH pore diameter calculated from the adsorption branch of the isotherm was 6.4 nm. These data showed that this material presents a mesoporous structure with a high surface area.

The X-ray diffraction powder pattern of the synthesized luminescent product is presented in Figure 6. In the SiDBM−Eu(DBM)$_2$ nanomaterial, a single diffraction peak appeared in the low 2θ region at 3.54, which is a characteristic peak of the formation of periodic hexagonal mesostructures.[22,39] This X-ray diffraction showed that SiDBM−Eu(DBM)$_2$ presents an interplanar distance of 2.49 nm.

The solid-state NMR of the ^{29}Si spectrum of SiDBM−Eu(DBM)$_2$ presented four typical peaks (Figure 7). The first one, at −48 ppm, which was assigned to the silicon atom of the silylating agent, bound to one hydroxyl group, forming the structure RSi(OSi)$_2$(OH), called the T3 signal. The second peak, at −58 ppm, was assigned to RSi(OSi)$_3$ (T4 signal).[38,40] T3 and T4 signals confirm that the organic groups are covalently bonded to the silica matrix. The other two peaks, at −96 and −104 ppm, were attributed to pure surface signals and were assigned, respectively, to (i) Si(OSi)$_3$OH, corresponding to the Q3 signal, and (ii) Si(OSi)$_4$, corresponding to the Q4 signal.[38,40]

Important features related to the information about the immobilization of a pendant group on the inorganic framework of the SiDBM−Eu(DBM)$_2$ can be obtained through ^{13}C NMR spectrum in the solid state. Figure 8 shows this spectrum, which presented many characteristic peaks at 5.6, 19.9, 31.6, 45.0, 80.6, 137.1, and 189.0 ppm. These peaks are assigned to carbons of the pendant groups, which are numbered elements in the spectrum. Two peaks must be highlighted; the one at 80.6 ppm is related to the carbon of carbonyl bonded to metal ion, proving the complexation of Eu^{3+} by diketone, and the other one at 189.0 ppm is assigned to carbon C═O of diketone, which was not bonded to Eu^{3+}.

Figure 9 showed the excitation and emission spectra of Eu^{3+} in the SiDBM−Eu(DBM)$_2$ material, which were recorded at ambient temperature. The emission spectrum consists of the transitions $^5D_0 \rightarrow {}^7F_J$ ($J = 0-4$), which were dominated by the hypersensitive $^5D_0 \rightarrow {}^7F_2$ transition peaking at 612 nm, giving an intense red luminescence output for the sample. Such observation indicates that the Eu^{3+} is in a symmetry site without inversion center. The excitation spectrum shows an intense and broad band centered at 363 nm due to the energy transfer from the excited levels of the DBM ligand to Eu^{3+} by the "antenna effect" process.

Luminescence decay curves of Eu^{3+} related to the $^5D_0 \rightarrow {}^7F_2$ emission are presented in Figure 10 and shows the decay curves for SiDBM−Eu and SiDBM−Eu(DBM)$_2$. The $^5D_0$ excited-state lifetime of Eu^{3+} in SiDBM−Eu (0.310 ± 0.002

(36) Franke, O.; Schulz-Ekloff, G.; Rathousky, J.; Starek, J.; Zukal, A. *J. Chem. Soc., Chem. Commun.* **1993**, 724.
(37) Branton, P. J.; Hall, P. G.; Sing, K. S. W. *J. Chem. Soc., Chem. Commun.* **1993**, 1257.
(38) DeOliveira, E.; Prado, A. G. S. *J. Mol. Catal. A: Chem.* **2007**, *271*, 63.
(39) Ogawa, M.; Ikeue, K.; Anpo, M. *Chem. Mater.* **2001**, *13*, 2900.
(40) Zhang, X. H.; Zhao, N.; Wei, W.; Sun, Y. *Catal. Today* **2006**, *115*, 102.

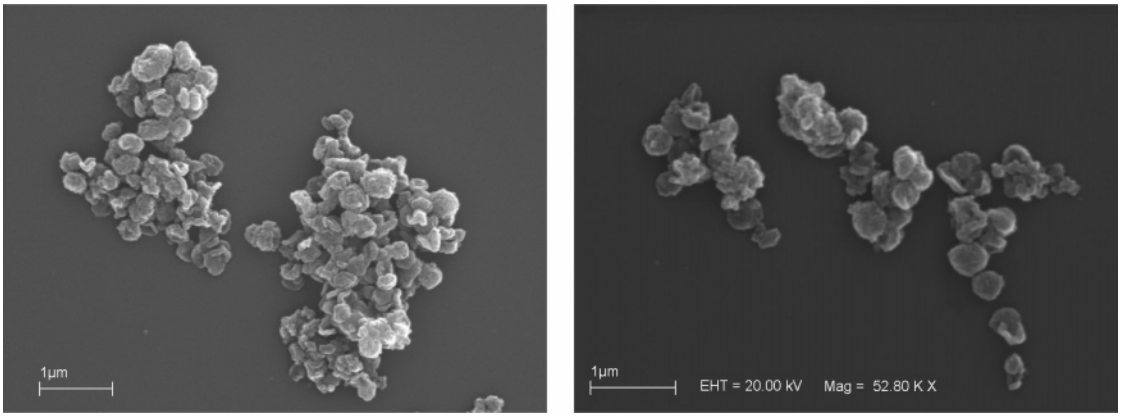

Figure 4. SEM images of SiDBM−Eu(DBM)$_2$.

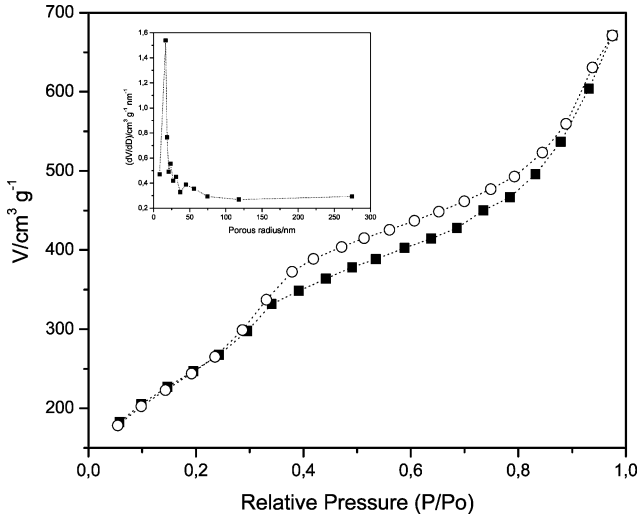

Figure 5. Nitrogen adsorption−desorption isotherms for the SiDBM−Eu(DBM)$_2$. Inset: the corresponding BJH pore size distribution curve.

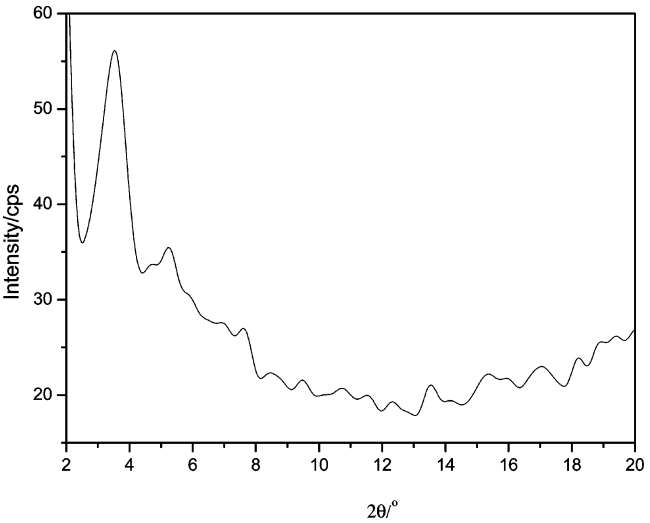

Figure 6. X-ray diffraction patterns of SiDBM−Eu(DBM)$_2$.

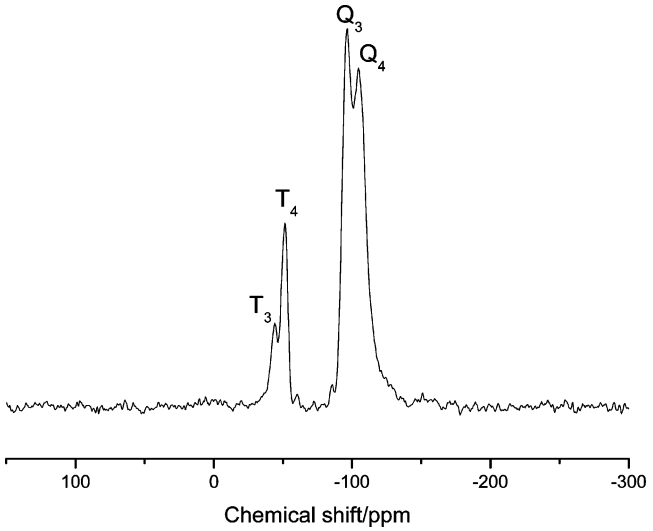

Figure 7. Solid-state ^{29}Si NMR spectra of SiDBM−Eu(DBM)$_2$.

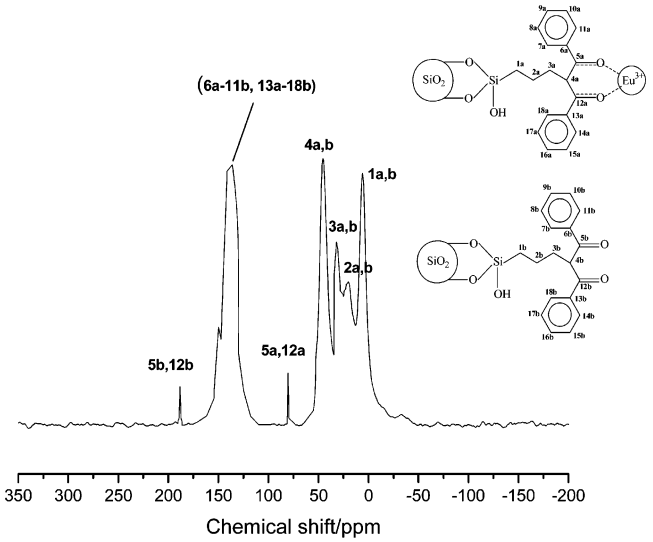

Figure 8. Solid-state ^{13}C NMR spectra of SiDBM−Eu(DBM)$_2$.

ms) is shorter than that of SiDBM−Eu(DBM)$_2$ (0.518 ± 0.001 ms). These low lifetime values are associated with the quenching by OH groups from the coordinated water molecules. The application of Horrocks equation[41] suggests the presence of an average of 4 H_2O molecules coordinated to Eu^{3+} in SiDBM−Eu and 2 H_2O molecules in SiDBM−Eu(DBM)$_2$. The replacement of water molecules in the first coordination sphere by DBM addition results in stronger emission and longer luminescence lifetime. The chromatic coordinates (CIE) are determined to be[42] $x = 0.66$ and $y = 0.34$. These values are very close to the ones considered as standard red emission ($x = 0.67$ and $y = 0.33$).[43]

(41) Horrocks, W. DeW., Jr.; Sudnick, D. R. *Acc. Chem. Res.* **1981**, *14*, 384.

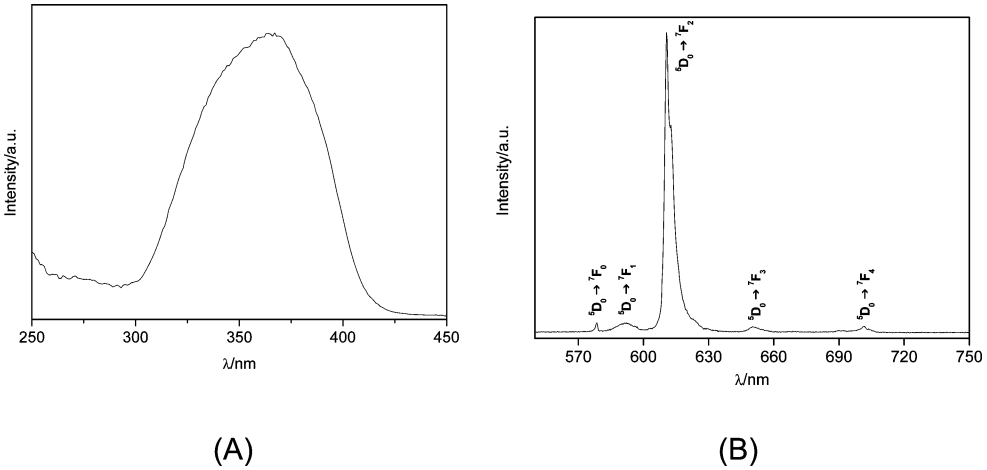

Figure 9. Excitation (A) and emission (B) spectra of SiDBM−Eu(DBM)$_2$: (λ_{exc} = 363 nm and λ_{em} = 612 nm), at room temperature.

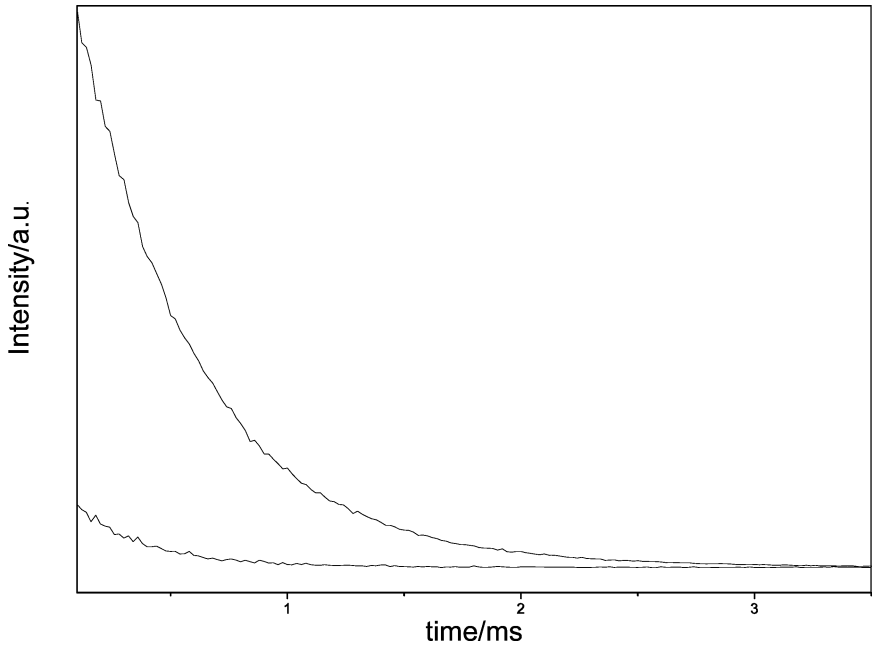

Figure 10. $^5D_0 \rightarrow {}^7F_2$ emission decay curves of SiDBM−Eu (a) and SiDBM−Eu(DBM)$_2$ (b) at room temperature.

Conclusion

Immobilization of DBM molecule in hexagonal mesoporous silica occurred by covalent bonding with silica structure. Eu^{3+} was coordinated by an average of three DBM molecules: one covalently bonded with silica and two unanchored. N_2 adsorption isotherm and X-ray diffraction confirmed that this luminescent material has ordered hexagonal mesoporosity. SEM images corroborates the formation of nanosized aggregates of this material, which presented excellent luminescent properties as well as intense and pure red emission (x = 0.66 and y = 0.34).

(42) Santa-Cruz, P. A.; Teles, F. S. Spectra Lux Software v.2.0, Ponto Quântico Nanodispositivos/RENAMI, 2003.
(43) Wang, Z.; Liang, H.; Gong, M.; Su, Q. *J. Alloys Compd.* **2007**, *432*, 308.

Acknowledgment. The authors acknowledge CAPES, CNPq, and FAPESP, for fellowships and financial support.

CM701997Y